the
is

Ing. Miroslav Hrstka

Evaluation of Fracture Mechanical Parameters for Bi-Piezo-Material Notch

EVALUATION OF FRACTURE MECHANICAL PARAMETERS FOR BI-PIEZO-MATERIAL NOTCH

STANOVENÍ LOMOVĚ MECHANICKÝCH PARAMETRŮ PRO BI-PIEZO-MATERIÁLOVÝ VRUB

ZKRÁCENÁ VERZE PH.D. THESIS

Contents

1 Introduction

Piezoelectric materials are extensively used as sensors or actuators in smart advanced structure design, as well as in many branches of technology. Commonly used piezoelectric materials are ceramics manufactured by conventional ceramic processing. In order to insure the reliability and structural integrity of electro-mechanical devices made from these materials, it is necessary to understand their mechanical behaviour. There has been a lot of research dealing with behaviour of piezoelectric ceramics.

The most significant work was done by Hwu in [1, 2, 3] and also in his monograph [4], where he summed up the previous research and expanded the Stroh formalism, the Key matrix, and the unified definition [5] to the piezoelectric media. Hirai et al. [6] and Abe et al. [7] applied the theory to certain bi-material notch configurations including determination of stress intensity factors by the Ψ-integral method.

Similar progress was carried out in extending the Lekhnitskii formalism in [8, 9]. General solution for piezoelectric anisotropic materials was derived in [10, 11, 12, 13]. Xu and Rajapakse [14], Chue and Chen [15] or Chen [16] investigated composite piezoelectric wedges and junctions, i.e. bi-materials composed from both piezoelectric and anisotropic materials.

Suo [17] developed the Lekhnitskii-Eshelby-Stroh formalism (LES formalism) for evaluating the stress singularity of anisotropic bi-material notches. However, its limit case – an interface crack – is primarily treated as the Hilbert problem, as can be seen in [18, 19, 20, 21, 22]. The present work employs the expanded LES formalism for piezoelectric continuum based on the studies [23, 24] and applies it to the problem of a piezoelectric bi-material notch and interface crack. In addition, both singular concentrator types are involved into one procedure that does not distinguish whether the value of the stress singularity exponent is complex or real, respectively.

In spite of a large number of studies related to the interfacial corners and interface cracks in jointed dissimilar piezoelectric materials there are only limited data concerning the asymptotic solutions around these concentrators. In particular, a transition between the oscillatory and non-oscillatory singularity as a function of the notch geometry and poling orientation for various dissimilar bi-materials has not been investigated yet. Hence, a wide range of notch geometries, material combinations, and poling orientations is considered here to shed some light on these problems.

2 Constitutive laws for piezoelectric materials

Material properties of linear piezoelectric materials are characterized by the elastic stiffness tensor $\mathbf{C}_E$ at constant electric field, piezoelectric tensor $\mathbf{e}$ and dielectric permittivity tensor $\boldsymbol{\omega}_\varepsilon$ at constant strain. The symmetry planes coincide with the global coordinate planes in the Cartesian coordinate system x_1, x_2, x_3.

The transversally isotropic symmetry is the most important one in the study of poled piezoelectric materials, but it is a special case of the more general monoclinic material whose elasticity and piezoelectricity matrices have the following structure:

$$\mathbf{C}_E = \begin{bmatrix} C_{11}^E & C_{12}^E & C_{13}^E & 0 & 0 & C_{16}^E \\ C_{12}^E & C_{22}^E & C_{23}^E & 0 & 0 & C_{26}^E \\ C_{13}^E & C_{23}^E & C_{33}^E & 0 & 0 & C_{36}^E \\ 0 & 0 & 0 & C_{44}^E & C_{45}^E & 0 \\ 0 & 0 & 0 & C_{45}^E & C_{55}^E & 0 \\ C_{16}^E & C_{26}^E & C_{36}^E & 0 & 0 & C_{66}^E \end{bmatrix},$$

$$\mathbf{e} = \begin{bmatrix} e_{11} & e_{12} & e_{13} & 0 & 0 & e_{16} \\ e_{21} & e_{22} & e_{23} & 0 & 0 & e_{26} \\ 0 & 0 & 0 & e_{34} & e_{35} & 0 \end{bmatrix}, \quad \boldsymbol{\omega}_\varepsilon = \begin{bmatrix} \omega_{11}^\varepsilon & \omega_{12}^\varepsilon & 0 \\ \omega_{12}^\varepsilon & \omega_{22}^\varepsilon & 0 \\ 0 & 0 & \omega_{33}^\varepsilon \end{bmatrix}. \tag{2.1}$$

It is worth noticing that the stiffness and permittivity matrices are symmetric, but the piezoelectric matrix is not. The directional properties of the matrices depend on the poling axis. Structure of the piezoelectric matrix depends on the poling direction, which can attain two limit configurations, either it coincides with x_1-axis or with x_2-axis. Between these states their structure corresponds to the above mentioned monoclinic one.

For an anisotropic and linearly electro-elastic solid, the constitutive laws between elastic field tensors (stresses σ_{ij} and strains ε_{ij}) and electric field vectors (electric displacements D_j and electric field E_j) can be then written in a matrix form as [1]

$$\begin{Bmatrix} \boldsymbol{\sigma} \\ \mathbf{D} \end{Bmatrix} = \begin{bmatrix} \mathbf{C}_E & \mathbf{e}^\mathsf{T} \\ \mathbf{e} & -\boldsymbol{\omega}_\varepsilon \end{bmatrix} \begin{Bmatrix} \boldsymbol{\varepsilon} \\ -\mathbf{E} \end{Bmatrix}, \quad \begin{Bmatrix} \boldsymbol{\varepsilon} \\ -\mathbf{E} \end{Bmatrix} = \begin{bmatrix} \mathbf{S}_D & \mathbf{g}^\mathsf{T} \\ \mathbf{g} & -\boldsymbol{\beta}_\sigma \end{bmatrix} \begin{Bmatrix} \boldsymbol{\sigma} \\ \mathbf{D} \end{Bmatrix}, \tag{2.2}$$

where

$$\boldsymbol{\sigma} = \begin{Bmatrix} \sigma_1 \\ \sigma_2 \\ \sigma_3 \\ \sigma_4 \\ \sigma_5 \\ \sigma_6 \end{Bmatrix} = \begin{Bmatrix} \sigma_{11} \\ \sigma_{22} \\ \sigma_{33} \\ \sigma_{23} \\ \sigma_{13} \\ \sigma_{12} \end{Bmatrix}, \quad \boldsymbol{\varepsilon} = \begin{Bmatrix} \varepsilon_1 \\ \varepsilon_2 \\ \varepsilon_3 \\ \varepsilon_4 \\ \varepsilon_5 \\ \varepsilon_6 \end{Bmatrix} = \begin{Bmatrix} \varepsilon_{11} \\ \varepsilon_{22} \\ \varepsilon_{33} \\ 2\varepsilon_{23} \\ 2\varepsilon_{13} \\ 2\varepsilon_{12} \end{Bmatrix},$$

$$\mathbf{E} = \begin{Bmatrix} E_1 \\ E_2 \\ E_3 \end{Bmatrix}, \quad \mathbf{D} = \begin{Bmatrix} D_1 \\ D_2 \\ D_3 \end{Bmatrix}. \tag{2.3}$$

The superscript T denotes matrix transposition. The matrices $\mathbf{C}_E$, $\mathbf{S}_D$, $\mathbf{e}$, $\mathbf{g}$, $\boldsymbol{\omega}_\varepsilon$ and $\boldsymbol{\beta}_\sigma$ fulfil the relations

$$\begin{bmatrix} \mathbf{C}_E & \mathbf{e}^\mathsf{T} \\ \mathbf{e} & -\boldsymbol{\omega}_\varepsilon \end{bmatrix} \begin{bmatrix} \mathbf{S}_D & \mathbf{g}^\mathsf{T} \\ \mathbf{g} & -\boldsymbol{\beta}_\sigma \end{bmatrix} = \mathbf{I}, \tag{2.4}$$

where the matrix $\mathbf{I}$ is the unit matrix of dimension 9×9. Let us designate the principal material coordinate system as x_i^*, in which we assemble the stiffness, piezoelectric and permittivity matrices and perform their inverse by (2.4) to obtain compliance matrix $\mathbf{S}_D^*$, piezoelectric matrix $\mathbf{g}^*$ and non-permittivities $\boldsymbol{\beta}_\sigma^*$. Then, the compliance and piezoelectric matrix and dielectric constants of the piezoelectric material transform as follows

$$\mathbf{S}_D = \left(\mathbf{K}^{-1}\right)^\mathsf{T} \mathbf{S}_D^* \mathbf{K}^{-1}, \quad \mathbf{g} = \boldsymbol{\Omega}\mathbf{g}^*\mathbf{K}^{-1}, \quad \boldsymbol{\beta}_\sigma = \boldsymbol{\Omega}\boldsymbol{\beta}_\sigma^*\boldsymbol{\Omega}^{-1}, \tag{2.5}$$

where the transformation matrices $\mathbf{K}$ and $\boldsymbol{\Omega}$ are defined by

$$\mathbf{K} = \begin{bmatrix} \cos^2\theta & \sin^2\theta & 0 & 0 & 0 & 2\cos\theta\sin\theta \\ \sin^2\theta & \cos^2\theta & 0 & 0 & 0 & -2\cos\theta\sin\theta \\ 0 & 0 & 1 & 0 & 0 & 0 \\ 0 & 0 & 0 & \cos\theta & -\sin\theta & 0 \\ 0 & 0 & 0 & \sin\theta & \cos\theta & 0 \\ -\cos\theta\sin\theta & \cos\theta\sin\theta & 0 & 0 & 0 & \cos^2\theta - \sin^2\theta \end{bmatrix}, \tag{2.6}$$

$$\boldsymbol{\Omega} = \begin{bmatrix} \cos\theta & \sin\theta & 0 \\ -\sin\theta & \cos\theta & 0 \\ 0 & 0 & 1 \end{bmatrix}. \tag{2.7}$$

The angle θ defines a rotation about x_3 axis in counter-clockwise direction and physically refers to the poling direction of the material. With respect to the material symmetry, the monoclinic materials with the symmetry axis parallel to $x_3 = 0$ are considered. Under the assumption that external

loads are parallel to a plane defined by $x_3 = 0$, only the in-plane field is investigated.

Except for the reduction of independent coordinates to x_1 and x_2, an important simplification in the decoupling of the plane fields is the rank reduction of the matrices (2.1) of the constitutive laws, which can be written as

$$
\left\{ \begin{array}{c} \boldsymbol{\sigma} \\ \mathbf{D} \end{array} \right\} = \begin{bmatrix} \mathbf{C}_E^0 & \mathbf{e}^{0\mathsf{T}} \\ \mathbf{e}^0 & -\boldsymbol{\omega}_\varepsilon^0 \end{bmatrix} \left\{ \begin{array}{c} \boldsymbol{\varepsilon} \\ -\mathbf{E} \end{array} \right\}, \quad \left\{ \begin{array}{c} \boldsymbol{\varepsilon} \\ -\mathbf{E} \end{array} \right\} = \begin{bmatrix} \hat{\mathbf{S}}'_D & \hat{\mathbf{g}}'^{\mathsf{T}} \\ \hat{\mathbf{g}}' & -\hat{\boldsymbol{\beta}}'_\sigma \end{bmatrix} \left\{ \begin{array}{c} \boldsymbol{\sigma} \\ \mathbf{D} \end{array} \right\}, \qquad (2.8)
$$

where

$$
\boldsymbol{\sigma} = \left\{ \begin{array}{c} \sigma_1 \\ \sigma_2 \\ \sigma_6 \end{array} \right\} \quad \boldsymbol{\varepsilon} = \left\{ \begin{array}{c} \varepsilon_1 \\ \varepsilon_2 \\ \varepsilon_6 \end{array} \right\} \quad \mathbf{E} = \left\{ \begin{array}{c} E_1 \\ E_2 \end{array} \right\}, \quad \mathbf{D} = \left\{ \begin{array}{c} D_1 \\ D_2 \end{array} \right\} \qquad (2.9)
$$

and

$$
\mathbf{C}_E^0 = \begin{bmatrix} C_{11}^E & C_{12}^E & C_{16}^E \\ C_{12}^E & C_{22}^E & C_{26}^E \\ C_{16}^E & C_{26}^E & C_{66}^E \end{bmatrix}, \quad \mathbf{e}^0 = \begin{bmatrix} e_{11} & e_{12} & e_{16} \\ e_{21} & e_{22} & e_{26} \end{bmatrix}, \quad \boldsymbol{\omega}_\varepsilon^0 = \begin{bmatrix} \omega_{11}^\varepsilon & \omega_{12}^\varepsilon \\ \omega_{21}^\varepsilon & \omega_{22}^\varepsilon \end{bmatrix}, \quad (2.10)
$$

$$
\hat{\mathbf{S}}'_D = \begin{bmatrix} \hat{S}_{11}'^D & \hat{S}_{12}'^D & \hat{S}_{16}'^D \\ \hat{S}_{12}'^D & \hat{S}_{22}'^D & \hat{S}_{26}'^D \\ \hat{S}_{16}'^D & \hat{S}_{26}'^D & \hat{S}_{66}'^D \end{bmatrix}, \quad \hat{\mathbf{g}}' = \begin{bmatrix} \hat{g}_{11}' & \hat{g}_{12}' & \hat{g}_{16}' \\ \hat{g}_{21}' & \hat{g}_{22}' & \hat{g}_{26}' \end{bmatrix}, \quad \hat{\boldsymbol{\beta}}'_\sigma = \begin{bmatrix} \hat{\beta}_{11}'^\sigma & \hat{\beta}_{12}'^\sigma \\ \hat{\beta}_{12}'^\sigma & \hat{\beta}_{22}'^\sigma \end{bmatrix}. \quad (2.11)
$$

The constitutive laws (2.8) are the in-plane part of the generalized plain strain and short circuit form of the constitutive laws in (2.2) also known as e-type and g-type, respectively. The reduced elements of the matrices in (2.8) are evaluated from the matrices in (2.2) under the assumption that $\varepsilon_3 = 0$ and $E_3 = 0$. This leads to the expressions

$$
\hat{S}_{ij}'^D = \hat{S}_{ij}^D + \frac{\hat{g}_{3i}\hat{g}_{3j}}{\hat{\beta}_{33}^\sigma} = \hat{S}_{ji}'^D, \quad \hat{g}_{ij}' = \hat{g}_{ij} - \frac{\hat{\beta}_{3i}^\sigma \hat{g}_{3j}}{\hat{\beta}_{33}^\sigma}, \quad \hat{\beta}_{ij}'^\sigma = \hat{\beta}_{ij}^\sigma - \frac{\hat{\beta}_{3i}^\sigma \hat{\beta}_{3j}^\sigma}{\hat{\beta}_{33}^\sigma} = \hat{\beta}_{ji}'^\sigma,
$$
$$(2.12)$$

in which

$$
\hat{S}_{ij}^D = S_{ij}^D - \frac{S_{3i}^D S_{3j}^D}{S_{33}^D} = \hat{S}_{ji}^D, \quad \hat{g}_{ij} = g_{ij} - \frac{g_{i3}S_{3j}^D}{S_{33}^D}, \quad \hat{\beta}_{ij}^\sigma = \beta_{ij}^\sigma + \frac{g_{i3}g_{j3}}{S_{33}^D} = \hat{\beta}_{ji}^\sigma
$$
$$(2.13)$$

for $i,j \neq 3$. There are more plane generalisations of the piezoelectricity, see [1], which are not discussed here.

3 Stress singularity of piezoelectric bi-material notch and interface crack

Typical representatives of non-degenerate ferroelectric materials are lead zirconate titanate – PZT-4, PZT-5H, PZT-6B, PZT-7, PZT-7A, barium titanate BaTiO$_3$, or zinc oxide ZnO. These functional ceramics possess the actuating strain (maximal to 0.2%), the high stiffness and the high response. In that case the in-plane and anti-plane fields can be decoupled when proper orientations are considered.

The in-plane problem of the stress singularity at the sharp notch composed of the two monoclinic piezoelectric materials is characterized by two generally complex exponents $\delta_1 - 1$, $\delta_2 - 1$ and one real exponent $\delta_3 - 1$. The resulting displacements and stresses are obtained as the superposition of these particular singular contributions weighted by the generally complex amplitudes. The amplitudes are introduced in the similar manner as for a crack and referred to as the generalized stress intensity factors (GSIFs). To start with, the following vectors are introduced

$$\mathbf{u}(z) = \mathbf{A}\mathbf{Z}^\delta \mathbf{v} + \overline{\mathbf{A}\mathbf{Z}}^\delta \mathbf{w}, \tag{3.1a}$$

$$\mathbf{T}(z) = \mathbf{L}\mathbf{Z}^\delta \mathbf{v} + \overline{\mathbf{L}\mathbf{Z}}^\delta \mathbf{w}, \tag{3.1b}$$

where

$$\mathbf{u} = \begin{Bmatrix} u_1 \\ u_2 \\ \phi \end{Bmatrix}, \quad \mathbf{T} = \begin{Bmatrix} T_1 \\ T_2 \\ T_D \end{Bmatrix},$$

$$\mathbf{A} = \begin{bmatrix} a_{11} & a_{12} & a_{13} \\ a_{21} & a_{22} & a_{23} \\ a_{31} & a_{32} & a_{33} \end{bmatrix}, \quad \mathbf{L} = \begin{bmatrix} -\mu_1 & -\mu_2 & -\mu_3\xi_3 \\ 1 & 1 & \xi_3 \\ -\xi_1 & -\xi_2 & -1 \end{bmatrix}, \tag{3.2}$$

where the elements of the matrices $\mathbf{A}$ and $\mathbf{L}$ are defined as ([9], [10], [13], [15], [25])

$$
\begin{aligned}
a_{1k} &= \mu_k^2 \hat{S}_{11}'^D + \hat{S}_{12}'^D - \mu_k \hat{S}_{16}'^D + \xi_k \left(\mu_k \hat{g}_{11}' - \hat{g}_{21}' \right), \quad (k = 1,2) \\
a_{2k} &= \left[\mu_k^2 \hat{S}_{12}'^D + \hat{S}_{22}'^D - \mu_k \hat{S}_{26}'^D + \xi_k \left(\mu_k \hat{g}_{12}' - \hat{g}_{22}' \right) \right] / \mu_k, \quad (k = 1,2) \\
a_{3k} &= \left[\mu_k^2 \hat{g}_{21}' + \hat{g}_{22}' - \mu_k \hat{g}_{26}' + \xi_k \left(-\mu_k \hat{\beta}_{12}'^\sigma + \hat{\beta}_{22}'^\sigma \right) \right] / \mu_k, \quad (k = 1,2) \\
a_{13} &= \left(\mu_3^2 \hat{S}_{11}'^D + \hat{S}_{12}'^D - \mu_3 \hat{S}_{16}'^D \right) \xi_3 + \mu_3 \hat{g}_{11}' - \hat{g}_{21}', \\
a_{23} &= \left[\left(\mu_3^2 \hat{S}_{12}'^D + \hat{S}_{22}'^D - \mu_3 \hat{S}_{26}'^D \right) \xi_3 + \mu_3 \hat{g}_{12}' - \hat{g}_{22}' \right] / \mu_3, \\
a_{33} &= \left[\left(\mu_3^2 \hat{g}_{21}' + \hat{g}_{22}' - \mu_3 \hat{g}_{26}' \right) \xi_3 - \mu_3 \hat{\beta}_{12}'^\sigma + \hat{\beta}_{22}'^\sigma \right] / \mu_3,
\end{aligned} \tag{3.3}
$$

$$\xi_k = -\frac{l_2(\mu_k)m_3(\mu_k)}{\rho_2(\mu_k)l_2(\mu_k)}, \quad (k=1,2),$$

$$\xi_k = -\frac{l_2(\mu_k)m_3(\mu_k)}{l_2(\mu_k)l_4(\mu_k)}, \quad (k=3),$$

(3.4)

where μ_i, $i = 1,2,3$ are the material eigenvalues. The parameter ϕ is the electric potential, T_1, T_2 and T_D are the components of the resulting tractions and the electric charge q along the semi-infinite line passing through the origin of the coordinate system x_1x_2. Then the vectors $\mathbf{u}$ and $\mathbf{T}$ at the tip of a piezoelectric bi-material wedge have the form [24]

$$\mathbf{u}(r,\theta) = H_1 r^{\delta_1}\boldsymbol{\eta}_1(\theta) + H_2 r^{\delta_2}\boldsymbol{\eta}_2(\theta) + H_3 r^{\delta_3}\boldsymbol{\eta}_3(\theta),$$

$$\mathbf{T}(r,\theta) = H_1 r^{\delta_1}\boldsymbol{\lambda}_1(\theta) + H_2 r^{\delta_2}\boldsymbol{\lambda}_2(\theta) + H_3 r^{\delta_3}\boldsymbol{\lambda}_3(\theta),$$

(3.5)

where H_i are generalized stress intensity factors, r and θ are polar coordinates, see Fig. 4.1, and

$$\boldsymbol{\eta}_i(\theta) = \mathbf{A}\mathbf{Z}^{\delta_i}(\theta)\mathbf{v}_i + \overline{\mathbf{A}}\,\overline{\mathbf{Z}}^{\delta_i}(\theta)\mathbf{w}_i,$$

$$\boldsymbol{\lambda}_i(\theta) = \mathbf{L}\mathbf{Z}^{\delta_i}(\theta)\mathbf{v}_i + \overline{\mathbf{L}}\,\overline{\mathbf{Z}}^{\delta_i}(\theta)\mathbf{w}_i.$$

(3.6)
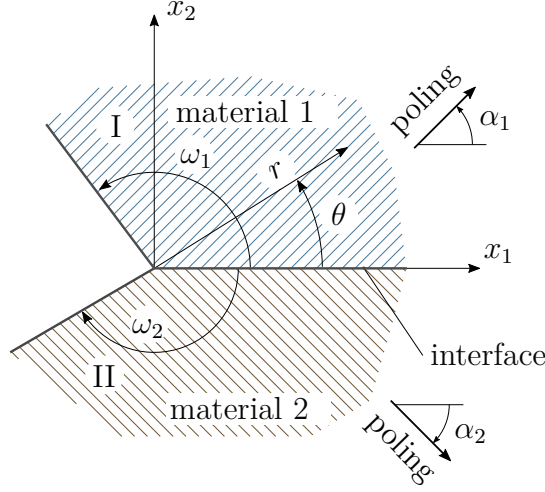
Fig. 4.1: Geometry of a bi-material notch characterized by two regions I and II. The notch faces are defined by angles ω_1 and ω_2. The bi-material interface is always considered at $\theta = 0$. The angles α_1 and α_2 denote poling directions of the materials I and II, respectively.

4 Formulation of singularity eigenvalue problem

In the previous sections, fundamental matrices were defined as functions of the stress and electric displacement singularity exponent δ, which is a root of the characteristic equation for a notch geometry and notch flanks prescribed boundary conditions. Considering a bi-material notch as illustrated in Fig. 4.1, where each wedge occupies the region $0 < \theta < \omega_1$ or $\omega_2 < \theta < 0$, traction free and impermeable (charge free) notch faces impose the following boundary conditions:

$$\begin{aligned} \mathbf{T}^{\mathrm{I}}(\omega_1) &= 0, \\ \mathbf{T}^{\mathrm{II}}(\omega_2) &= 0. \end{aligned} \tag{4.1}$$

The boundary conditions (4.1) imply that normal electrical displacement is zero on the notch faces, i.e. $D_n^{\mathrm{I}} = D_n^{\mathrm{II}} = 0$. This electric boundary condition is still debated, but it requires much simpler mathematical treatment and the zero surface charge condition is not violated, when one material has significantly higher permittivity than the second one, e.g. a piezoelectric ceramic in a contact with air [26]. The bi-material interface is assumed to be coincident with x_1 axis. The displacement and traction continuity conditions are prescribed along the interface $\theta = 0$ as

$$\begin{aligned} \mathbf{u}^{\mathrm{I}}(0) &= \mathbf{u}^{\mathrm{II}}(0), \\ \mathbf{T}^{\mathrm{I}}(0) &= \mathbf{T}^{\mathrm{II}}(0). \end{aligned} \tag{4.2}$$

11

Let us consider a bi-material notch composed of two monoclinic materials, with principal material symmetry arbitrary oriented in the plane $x_3 = 0$. By substituting vector functions $\boldsymbol{\lambda}(\theta)$ and $\boldsymbol{\eta}(\theta)$ from (3.6) into (4.1) and (4.2), one gets for the exponent δ eight homogeneous algebraic equations, which can be written in the matrix form as

$$\begin{bmatrix} \mathbf{X}_1^{\mathrm{I}} & \overline{\mathbf{X}}_1^{\mathrm{I}} & \mathbf{0} & \mathbf{0} \\ \mathbf{0} & \mathbf{0} & \mathbf{X}_2^{\mathrm{II}} & \overline{\mathbf{X}}_2^{\mathrm{II}} \\ \mathbf{B}_0^{\mathrm{I}} & -\overline{\mathbf{B}}_0^{\mathrm{I}} & -\mathbf{B}_0^{\mathrm{II}} & \overline{\mathbf{B}}_0^{\mathrm{II}} \\ \mathbf{I} & \mathbf{I} & -\mathbf{I} & -\mathbf{I} \end{bmatrix} \left\{ \begin{array}{c} \mathbf{L}^{\mathrm{I}}\mathbf{v}^{\mathrm{I}} \\ \overline{\mathbf{L}}^{\mathrm{I}}\mathbf{w}^{\mathrm{I}} \\ \mathbf{L}^{\mathrm{II}}\mathbf{v}^{\mathrm{II}} \\ \overline{\mathbf{L}}^{\mathrm{II}}\mathbf{w}^{\mathrm{II}} \end{array} \right\} = \mathbf{0}, \tag{4.3}$$

$$\mathbf{X}_j = \mathbf{L}\mathbf{Z}_j^{\delta}\left(\omega_j\right)\left(\mathbf{L}\right)^{-1}, \quad \overline{\mathbf{X}}_j = \overline{\mathbf{L}}\overline{\mathbf{Z}}_j^{\delta}\left(\omega_j\right)\left(\overline{\mathbf{L}}\right)^{-1}, \quad (j = 1,2) \tag{4.4a}$$

$$\mathbf{B}_0 = i\mathbf{A}\mathbf{L}^{-1}, \quad \overline{\mathbf{B}}_0 = -i\overline{\mathbf{A}}\overline{\mathbf{L}}^{-1}, \tag{4.4b}$$

$$\mathbf{Y}_j = \overline{\mathbf{X}}_j^{-1}\mathbf{X}_j, \quad (j = 1,2), \tag{4.4c}$$

where $\mathbf{0}$ denotes 3×3 zero matrix on the left-hand side and 12×1 zero vector on the right-hand side of the equation (4.3). The algebraic system of the twelve equations (4.3) can always be reduced to the algebraic system of three equations only. Let us introduce a vector

$$\mathbf{L}_a^{\mathrm{I}}\mathbf{v}_a^{\mathrm{I}} = \frac{1}{2}\left(\mathbf{L}^{\mathrm{I}}\mathbf{v}^{\mathrm{I}} + \overline{\mathbf{L}}^{\mathrm{I}}\mathbf{w}^{\mathrm{I}}\right), \tag{4.5}$$

where index a stands for an average value of both eigenvectors $\mathbf{L}^{\mathrm{I}}\mathbf{v}^{\mathrm{I}}$ and $\mathbf{L}^{\mathrm{I}}\mathbf{w}^{\mathrm{I}}$ with no physical meaning. Then the homogeneous algebraic system (4.3) can be reduced to

$$\mathbf{K}\left(\mathbf{I} - \mathbf{Y}_1^{\mathrm{I}}\right)^{-1}2\mathbf{L}_a^{\mathrm{I}}\mathbf{v}_a^{\mathrm{I}} = \mathbf{0}, \tag{4.6}$$

where

$$\mathbf{K} = \mathbf{B}_0^{\mathrm{I}} + \overline{\mathbf{B}}_0^{\mathrm{I}}\mathbf{Y}_1^{\mathrm{I}} - \left(\mathbf{B}_0^{\mathrm{II}} + \overline{\mathbf{B}}_0^{\mathrm{II}}\mathbf{Y}_2^{\mathrm{II}}\right)\left(\mathbf{I} - \mathbf{Y}_2^{\mathrm{II}}\right)^{-1}\left(\mathbf{I} - \mathbf{Y}_1^{\mathrm{I}}\right). \tag{4.7}$$

The matrix (4.7) can be found also in [27] and [28], but only for the case of pure anisotropy and the real exponent δ. To get a non-trivial solution of (4.6), the following relation for any δ must hold:

$$\det\left[\mathbf{K}(\delta)\right] = 0, \tag{4.8}$$

which leads to a nonlinear characteristic equation, which has unlimited number of solutions δ_i. In the literature the solution δ_i is sometimes called

eigenvalue. Since from the physical point of view the strain energy cannot be unbounded, the values satisfying the condition $0 < \Re\{\delta_i\} < 1$ have to be considered. The corresponding eigenvectors $\mathbf{v}_i^{\mathrm{I}}$, $\mathbf{v}_i^{\mathrm{II}}$ and $\mathbf{w}_i^{\mathrm{I}}$, $\mathbf{w}_i^{\mathrm{II}}$ are evaluated from the expressions

$$
\begin{aligned}
\mathbf{v}_i^{\mathrm{I}} &= \left(\mathbf{L}^{\mathrm{I}}\right)^{-1}\left(\mathbf{I} - \mathbf{Y}_1^{\mathrm{I}}\right)^{-1} 2\mathbf{L}_a^{\mathrm{I}}\mathbf{v}_a^{\mathrm{I}}, \\
\mathbf{v}_i^{\mathrm{II}} &= \left(\mathbf{L}^{\mathrm{II}}\right)^{-1}\left(\mathbf{I} - \mathbf{Y}_2^{\mathrm{II}}\right)^{-1}\left(\mathbf{I} - \mathbf{Y}_1^{\mathrm{I}}\right)\mathbf{L}^{\mathrm{I}}\mathbf{v}_i^{\mathrm{I}}, \\
\mathbf{w}_i^{\mathrm{I}} &= -\left(\overline{\mathbf{L}}^{\mathrm{I}}\right)^{-1}\mathbf{Y}_1^{\mathrm{I}}\mathbf{L}^{\mathrm{I}}\mathbf{v}_i^{\mathrm{I}}, \\
\mathbf{w}_i^{\mathrm{II}} &= -\left(\overline{\mathbf{L}}^{\mathrm{II}}\right)^{-1}\mathbf{Y}_2^{\mathrm{II}}\mathbf{L}^{\mathrm{II}}\mathbf{v}_i^{\mathrm{II}}.
\end{aligned}
\tag{4.9}
$$

The exponent δ_i and corresponding eigenvectors $\mathbf{v}_i^{\mathrm{I}}$, $\mathbf{v}_i^{\mathrm{II}}$ and $\mathbf{w}_i^{\mathrm{I}}$, $\mathbf{w}_i^{\mathrm{II}}$ determine the so-called regular solution. It can be proved, see [29], that exponent $\hat{\delta}_i = -\delta_i$ also satisfies (4.8). This so-called auxiliary solution is only a mathematical tool allowing to evaluate the GSIFs via the Betti theorem-based path-independent integral introduced hereafter. It represents a stress field at the notch tip whose singularity is stronger then the regular one and hence exhibits unbounded energy. By reinserting $\hat{\delta}_i$ into (4.6) and by employing (4.9), the corresponding auxiliary eigenvector $\hat{\mathbf{v}}_i^{\mathrm{I}}$ can be evaluated as well as the remaining auxiliary eigenvectors $\hat{\mathbf{v}}_i^{\mathrm{II}}$, $\hat{\mathbf{w}}_i^{\mathrm{I}}$ and $\hat{\mathbf{w}}_i^{\mathrm{II}}$.

It is worth noting that the disproportion of the elastic, piezoelectric and permittivity constants causes that the matrices appearing in the constitutive laws (2.8) are ill-conditioned and hence usual numerical procedures for the evaluation of the eigenvalues and eigenvectors of the matrix $\mathbf{K}(\delta_i)$ often give erroneous results. For this reason, it is suitable to use an alternative method of the evaluation of the eigenvectors $\mathbf{v}_i^{\mathrm{I}}$, $\mathbf{v}_i^{\mathrm{II}}$, $\mathbf{w}_i^{\mathrm{I}}$, $\mathbf{w}_i^{\mathrm{II}}$ and their auxiliary complements $\hat{\mathbf{v}}_i^{\mathrm{I}}$, $\hat{\mathbf{v}}_i^{\mathrm{II}}$, $\hat{\mathbf{w}}_i^{\mathrm{I}}$, $\hat{\mathbf{w}}_i^{\mathrm{II}}$. By substituting δ_i or $\hat{\delta}_i$ into (4.6) we get

$$
\mathbf{K}^*(\delta_i)\mathbf{v}_i^* = \mathbf{0}, \quad (i = 1,2,3),
\tag{4.10}
$$

where

$$
\mathbf{K}^* = \mathbf{K}\left(\mathbf{I} - \mathbf{Y}_1^{\mathrm{I}}\right)^{-1}, \quad \text{and} \quad \mathbf{v}_i^* = 2\mathbf{L}_a^{\mathrm{I}}\mathbf{v}_a^{\mathrm{I}}.
\tag{4.11}
$$

Equation (4.10) can be expressed in a matrix form as

$$
\begin{bmatrix} K_{11}^{i*} & K_{12}^{i*} & K_{13}^{i*} \\ K_{21}^{i*} & K_{22}^{i*} & K_{23}^{i*} \\ K_{31}^{i*} & K_{32}^{i*} & K_{33}^{i*} \end{bmatrix} \begin{Bmatrix} v_1^{i*} \\ v_2^{i*} \\ v_3^{i*} \end{Bmatrix} = \begin{Bmatrix} 0 \\ 0 \\ 0 \end{Bmatrix}.
\tag{4.12}
$$

Because of the singularity of the matrix $\mathbf{K}^*(\delta_i)$, one vector component is chosen, i.e. $v_3^{i*} = 1$, to eliminate one row of $\mathbf{K}^*(\delta_i)$. The system (4.12) is

then reordered as

$$\begin{bmatrix} K_{11}^{i*} & K_{12}^{i*} \\ K_{21}^{i*} & K_{22}^{i*} \end{bmatrix} \begin{Bmatrix} v_1^{i*} \\ v_2^{i*} \end{Bmatrix} = \begin{Bmatrix} -K_{13}^{i*} \\ -K_{23}^{i*} \end{Bmatrix}. \tag{4.13}$$

The remaining vector components can be now solved as an ordinary system of two linear equations. In connection with the LES formalism we can define

$$2\mathbf{L}_a^{\mathrm{I}} \mathbf{v}_a^{\mathrm{I}} = \begin{Bmatrix} v_1^{i*} \\ v_2^{i*} \\ 1 \end{Bmatrix}. \tag{4.14}$$

Finally it is convenient to evaluate the eigenvector $\mathbf{v}_i^{\mathrm{I}}$ from the normalized vector $\mathbf{L}^{\mathrm{I}} \mathbf{v}_i^{\mathrm{I}}$ according to the standard numerical algorithms

$$\mathbf{L}^{\mathrm{I}} \mathbf{v}_i^{\mathrm{I}} = \frac{\left(\mathbf{I} - \mathbf{Y}_1^{\mathrm{I}}\right)^{-1} 2\mathbf{L}_a^{\mathrm{I}} \mathbf{v}_a^{\mathrm{I}}}{\left\|\left(\mathbf{I} - \mathbf{Y}_1^{\mathrm{I}}\right)^{-1} 2\mathbf{L}_a^{\mathrm{I}} \mathbf{v}_a^{\mathrm{I}}\right\|}. \tag{4.15}$$

The remaining eigenvectors $\mathbf{v}_i^{\mathrm{II}}$, $\mathbf{w}_i^{\mathrm{I}}$ and $\mathbf{w}_i^{\mathrm{II}}$ are evaluated using $(4.9)_2-$ $(4.9)_4$.

5 Determination of generalized stress intensity factors

GSIFs determine the amplitude of the displacements, electric potential, stresses and electrical displacements characterized by normalized shape functions (3.6). In the present work, GSIFs are determined by using the Ψ-integral method, which was firstly introduced by Sinclair et al. [30], Vu-Quoc and Tran [31], and deeply investigated by Hwu [4]. It is based on the Betti and Rayleigh reciprocal theorem [32]. Contrary to the J-integral, the path-independence of Ψ-integral is also preserved for multi-material stress concentrators. Neglecting the body forces, the Ψ-integral for a bi-material notch characterised by angles ω_1 and ω_2 becomes

$$\Psi(\mathbf{u},\hat{\mathbf{u}}_i) = \int_{\omega_2}^{\omega_1} \left(\mathbf{u}^{\mathsf{T}}\hat{\mathbf{t}}_i - \hat{\mathbf{u}}_i^{\mathsf{T}}\mathbf{t} \right) r \, \mathrm{d}\theta. \tag{5.1}$$

The vectors $\hat{\mathbf{u}}_i$ and $\hat{\mathbf{t}}_i$ are the auxiliary solutions to the displacements, tractions, electric potential and the charge and correspond to the exponent $\hat{\delta}_i = -\delta_i$. The auxiliary solutions are defined as

$$\hat{\mathbf{u}}_i(r,\theta) = r^{-\delta_i}\hat{\boldsymbol{\eta}}_i(\theta),$$
$$\hat{\mathbf{t}}_i(r,\theta) = -\frac{1}{r}\frac{\partial \hat{\mathbf{T}}_i(r,\theta)}{\partial \theta} = -r^{-\delta_i-1}\hat{\boldsymbol{\lambda}}_i'(\theta), \qquad (i = 1,2,3) \tag{5.2}$$

where $(.)'$ denotes the differentiation with respect to θ,

$$\hat{\boldsymbol{\eta}}_i(\theta) = \mathbf{A}\mathbf{Z}^{-\delta_i}(\theta)\hat{\mathbf{v}}_i + \overline{\mathbf{A}\mathbf{Z}}^{-\delta_i}(\theta)\hat{\mathbf{w}}_i,$$
$$\hat{\boldsymbol{\lambda}}_i'(\theta) = \mathbf{L}\left(\mathbf{Z}^{-\delta_i}(\theta)\right)'\hat{\mathbf{v}}_i + \overline{\mathbf{L}}\left(\overline{\mathbf{Z}}^{-\delta_i}(\theta)\right)'\hat{\mathbf{w}}_i \qquad (i = 1,2,3) \tag{5.3}$$

and

$$\left(\mathbf{Z}^{\delta}(\theta)\right)' = \mathrm{diag}\left[\delta R_1^{\delta-1}(\theta)\,\mathrm{e}^{i(\delta-1)\Psi_1(\theta)}\left[-\sin\theta + \mu_1\cos\theta\right],\right.$$
$$\delta R_2^{\delta-1}(\theta)\,\mathrm{e}^{i(\delta-1)\Psi_2(\theta)}\left[-\sin\theta + \mu_2\cos\theta\right], \tag{5.4}$$
$$\left.\delta R_3^{\delta-1}(\theta)\,\mathrm{e}^{i(\delta-1)\Psi_3(\theta)}\left[-\sin\theta + \mu_3\cos\theta\right]\right],$$

$$\left(\overline{\mathbf{Z}}^{\delta}(\theta)\right)' = \mathrm{diag}\left[\delta R_1^{\delta-1}(\theta)\,\mathrm{e}^{-i(\delta-1)\Psi_1(\theta)}\left[-\sin\theta + \overline{\mu}_1\cos\theta\right],\right.$$
$$\delta R_2^{\delta-1}(\theta)\,\mathrm{e}^{-i(\delta-1)\Psi_2(\theta)}\left[-\sin\theta + \overline{\mu}_2\cos\theta\right], \tag{5.5}$$
$$\left.\delta R_3^{\delta-1}(\theta)\,\mathrm{e}^{-i(\delta-1)\Psi_3(\theta)}\left[-\sin\theta + \overline{\mu}_3\cos\theta\right]\right].$$

The vectors $\mathbf{u}$ and $\mathbf{t}$ represent either the regular asymptotic or a full-field solution obtained numerically. In the first case, the vector $\mathbf{u}$ is given by

15

$(3.5)_1$ and the vector $\mathbf{t}$ is given by the derivative of $(3.5)_2$ with respect to θ,

$$\mathbf{t}(r,\theta) = -\frac{1}{r}\frac{\partial \mathbf{T}(r,\theta)}{\partial \theta} = -H_1 r^{\delta_1-1}\boldsymbol{\lambda}_1'(\theta) - H_2 r^{\delta_2-1}\boldsymbol{\lambda}_2'(\theta) - H_3 r^{\delta_3-1}\boldsymbol{\lambda}_3'(\theta),$$
(5.6)

where, taking into account $\delta = \delta_i$ in (5.4) and (5.5), one can write

$$\boldsymbol{\lambda}_i'(\theta) = \mathbf{L}\left(\mathbf{Z}^{\delta_i}(\theta)\right)' \mathbf{v}_i + \overline{\mathbf{L}}\left(\overline{\mathbf{Z}}^{\delta_i}(\theta)\right)' \mathbf{w}_i, \quad (i = 1,2,3).$$
(5.7)

Obviously, if the integration contour in the Ψ-integral shrinks to the notch tip, the full-field solution reduces to the asymptotic solution $(3.5)_1$ and (5.6). Since the regular and corresponding auxiliary solutions are orthogonal with respect to the integral (5.1), i.e.

$$\Psi\left(r^{\delta_j}\boldsymbol{\eta}_j(\theta), r^{-\delta_i}\hat{\boldsymbol{\eta}}_i(\theta)\right) = \begin{cases} \text{const} \neq 0 & \text{for} \quad i = j, \\ 0 & \text{for} \quad i \neq j, \end{cases}$$
(5.8)

the Ψ-integral computed along a path very close to the crack tip gives an important result for the GSIFs evaluation

$$\Psi\left(\mathbf{u}, r^{-\delta_i}\hat{\boldsymbol{\eta}}_i(\theta)\right) = \Psi\left(r^{\delta_i}\boldsymbol{\eta}_i(\theta), r^{-\delta_i}\hat{\boldsymbol{\eta}}_i(\theta)\right) = \\ = H_i \int_{\omega_2}^{\omega_1}\left(\boldsymbol{\eta}_i^{\mathsf{T}}(\theta)\hat{\boldsymbol{\lambda}}_i'(\theta) - \hat{\boldsymbol{\eta}}_i^{\mathsf{T}}(\theta)\boldsymbol{\lambda}_i'(\theta)\right) \mathrm{d}\theta,$$
(5.9)

which is independent on the radial coordinate r.

Making use of the Ψ-integral path-independence, the GSIFs can be computed if the right-hand side of equation (5.9) is put equal to the Ψ-integral computed along the remote contour which contains a full-field solution to the vectors $\mathbf{u}$ and $\mathbf{t}$. In the present work the full-field solution is approximated using FEM implemented in ANSYS software [33] and/or FEniCS 2018.1 [34]. The integration contour is chosen far away from the notch tip. Let us introduce the integral

$$\Psi\left(\mathbf{u}^{FEM}, r_c^{-\delta_i}\hat{\boldsymbol{\eta}}_i(\theta)\right) = \\ = \int_{\omega_2}^{\omega_1}\left(\left(\mathbf{u}^{\text{FEM}}\right)^{\mathsf{T}} r_c^{-\delta_i-1}\hat{\boldsymbol{\lambda}}_i'(\theta) + r_c^{-\delta_i}\hat{\boldsymbol{\eta}}_i^{\mathsf{T}}(\theta)\mathbf{t}^{\text{FEM}}\right) r_c \,\mathrm{d}\theta,$$
(5.10)

where r_c is the radius of the circular path remote from the notch singularity. Note that the signs follow from the orientation of the outward normal and the integration contour. The elements of the vector $\mathbf{u}^{\text{FEM}} = \left[u_1^{\text{FEM}}, u_2^{\text{FEM}}, \phi^{\text{FEM}}\right]^{\mathsf{T}}$ are the solution obtained by FEM, but elements of the

vector $\mathbf{t}^{\mathrm{FEM}}$ along the integrating contour have to be computed from the stresses using the Cauchy's formula $t_i = \sigma_{ij} n_j$, in a matrix form written as

$$\mathbf{t}^{\mathrm{FEM}} = \boldsymbol{\sigma}^{\mathrm{FEM}} \mathbf{n}, \tag{5.11}$$

where $\boldsymbol{\sigma}^{\mathrm{FEM}}$ is the two-dimensional generalized stress tensor and $\mathbf{n}$ is the outer normal to the domain enclosed by the circular integrating path of the radius r_c defined as

$$\boldsymbol{\sigma}^{\mathrm{FEM}} = \begin{bmatrix} \sigma_{11}^{\mathrm{FEM}} & \sigma_{12}^{\mathrm{FEM}} \\ \sigma_{21}^{\mathrm{FEM}} & \sigma_{22}^{\mathrm{FEM}} \\ D_1^{\mathrm{FEM}} & D_2^{\mathrm{FEM}} \end{bmatrix}, \quad \mathbf{n} = \begin{Bmatrix} \cos(\theta) \\ \sin(\theta) \end{Bmatrix}. \tag{5.12}$$

Applying the analogy with standard dot product of the vectors, the Ψ-integrals (5.9) and (5.10) project analytical and numerical solution of the same problem into the basis function of some dual function space generated by the auxiliary solutions (5.3). Hence both Ψ-integrals (5.9) and (5.10) are equal and the following relations hold

$$H_i = \frac{\Psi\left(\mathbf{u}^{\mathrm{FEM}}, r_c^{-\delta_i} \hat{\boldsymbol{\eta}}_i(\theta)\right)}{\Psi\left(r_c^{\delta_i} \boldsymbol{\eta}_i(\theta), r_c^{-\delta_i} \hat{\boldsymbol{\eta}}_i(\theta)\right)}, \quad (i = 1,2,3). \tag{5.13}$$

material constants		PZT-4	PZT-5H	PZT-6B	PZT-7A	BaTiO$_3$
C_{11}^E	$\times 10^{10}$ [Pa]	11.3	11.7	16.3	13.1	14.6
C_{12}^E	$\times 10^{10}$ [Pa]	7.43	5.30	6.00	7.42	6.60
C_{23}^E	$\times 10^{10}$ [Pa]	7.78	5.50	6.00	7.62	6.60
C_{22}^E	$\times 10^{10}$ [Pa]	13.9	12.6	16.8	14.8	15.0
C_{44}^E	$\times 10^{10}$ [Pa]	2.56	3.53	2.71	2.54	4.40
e_{11}	[Cm^{-2}]	13.8	23.3	7.10	9.50	17.5
e_{12}	[Cm^{-2}]	-6.98	-6.50	-0.90	-2.10	-4.35
e_{26}	[Cm^{-2}]	13.4	17.0	4.60	9.70	11.4
ω_{11}^ε	$\times 10^{-9}$ [C(Vm)$^{-1}$]	5.47	13.0	3.40	7.35	11.2
ω_{22}^ε	$\times 10^{-9}$ [C(Vm)$^{-1}$]	6.00	15.1	3.60	8.11	9.87

Tab. 6.1: Material properties of some transversally isotropic piezoelectric ceramics poled in x_1-direction [6, 7, 19].

bi-materials	δ_1	δ_2	oscillatory index ε	comparison with Ou and Wu [19]
PZT-5H/BaTiO$_3$	$0.5 + 0.01293i$	$0.5 - 0.01293i$	0.01293	0.0130
PZT-5H/PZT-6B	$0.5 + 0.02189i$	$0.5 - 0.02189i$	0.02189	0.0219
PZT-5H/PZT-7A[†]	$0.5 + 0.00697i$	$0.5 - 0.00697i$	0.00697	0.0069
PZT-6B/PZT-7A	$0.5 + 0.00547i$	$0.5 - 0.00547i$	0.00547	0.0055

[†] $\delta_{1,2} = 0.5 \pm 0.00697i$ computed by Hwu and Kuo [3] by using the expanded Stroh formalism

Tab. 6.2: Oscillatory indices of ε-class bi-materials and their comparison with results in [19].

6 Results and discussion

Let us consider a piezoelectric bi-material notch with local geometry and poling directions schematically illustrated in Fig. 4.1. Herein, the angles α_1, α_2 denote the poling directions. Elastic, piezoelectric and electric material characteristics are stated in Tab. 6.1.

Let us consider PZT-5H/BaTiO$_3$ as the material 1/material 2 combination and the bi-material notch geometry described by $\omega_1 = 120°$ and $\omega_2 = -180°$. In all of the following examples, poling direction is parallel with x_2-axis ($\alpha_1 = \alpha_2 = 90°$) if it is not specified otherwise.

Three real roots $\delta_1 = 0.5226$, $\delta_2 = 0.5770$ and $\delta_3 = 0.7462$ of the characteristic function (4.8) on the interval $0 < \Re\{\delta\} < 1$ were obtained. In the case of an interface crack ($\omega_1 = 180°$), there are two complex conjugate roots $\delta_1 = 0.5 + 0.01293i$, $\delta_2 = 0.5 - 0.01293i$ and the third root is real,

bi-materials	δ_1	δ_3	non-oscillatory index κ	comparison with Ou and Wu [19]
PZT-4/BaTiO$_3$	0.44914	0.55086	0.05086	0.0508
PZT-4/PZT-5H	0.45585	0.54415	0.04415	0.0442
PZT-4/PZT-6B	0.48316	0.51684	0.01684	0.0168
PZT-4/PZT-7A	0.47525	0.52475	0.02475	0.0247
PZT-6B/BaTiO$_3$	0.49039	0.50961	0.00961	0.0095
PZT-7A/BaTiO$_3$	0.47936	0.52064	0.02064	0.0206

Tab. 6.3: Non-oscillatory indices of κ-class bi-materials and their comparison with [19].

(a) PZT-5H/BaTiO$_3$.   (b) PZT-5H/PZT-4.
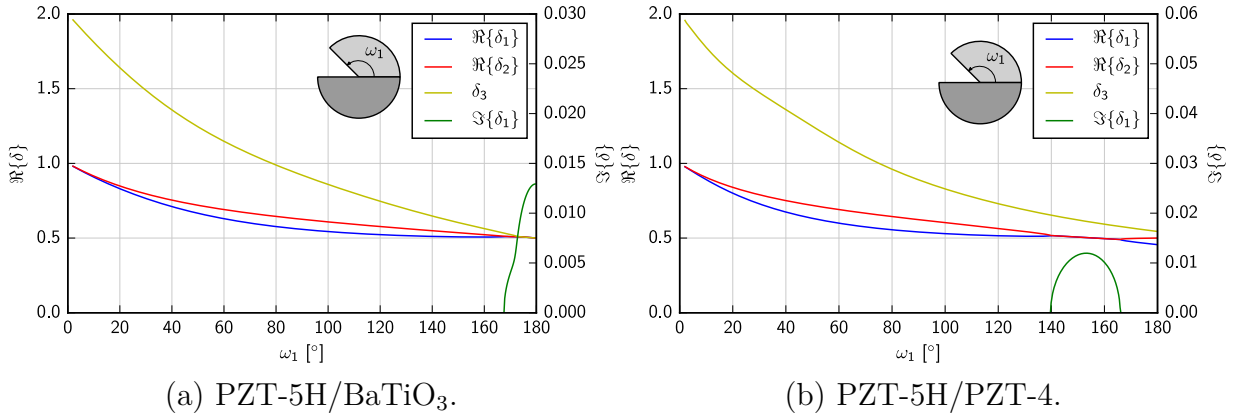
Fig. 6.1: The exponent δ_i dependence on the notch geometry ω_1. Poling directions are $\alpha_1 = 90°$, $\alpha_2 = 90°$.

$\delta_3 = 0.5$.

Different results are obtained when we consider an interface crack between PZT-5H and PZT-4 materials. Note that the crack faces are considered to be impermeable, i.e. free of electric charge. There are three real roots: $\delta_1 = 0.4558$, $\delta_2 = 0.5$ and $\delta_3 = 0.5442$. The disappearance of the oscillatory index ε is consistent with the results obtained by Ou and Wu [19], who investigated the interface crack in terms of the Hilbert problem, e.g. [17]. They found out that there are two types of singularities in the case of interface crack between two piezoelectric material – the oscillatory singularity when exponents have the oscillatory index ε or the non-oscillatory singularity with the parameter $i\kappa$. In the first case, the eigenvalues have the form

$$\delta_{1,2} = 0.5 \pm i\varepsilon, \qquad (6.1)$$

while in the latter case

$$\delta_{1,3} = 0.5 \pm i(i\kappa) = 0.5 \mp \kappa, \qquad (6.2)$$

which are real numbers. The bi-materials with an interface crack are then divided into two classes: ε-class and κ-class. Contrary to the Hilbert problem formulation used in [19], the employed procedure for solution of the eigenvalue problem (4.3) and (4.4) does not provide for κ-class bi-materials the parameter $i\kappa$ and the value 0.5 separately, but they are merged in the resulting roots δ of the characteristic function (4.8). When taking a look at the exponents for the PZT-5H/PZT-4 bi-material more closely, it can be seen that δ_1 and δ_3 are symmetric with respect to the $\delta_2 = 0.5$. Then the parameter κ can be extracted by subtracting the value 0.5 from δ_1 or δ_3, respectively. The obtained results of δ_1 and δ_2 for ε-class or δ_1 and δ_3 for κ-class bi-materials compared with the values reported in the literature are summarized in Tab. 6.2 and Tab. 6.3. The remaining exponents are always $\delta_3 = 0.5$ or $\delta_2 = 0.5$, respectively. Tab. 6.3 gives the parameter κ extracted from the obtained exponent using Eq. (6.2). One can see that the all received values of δ_1 and δ_2 or δ_3 coincide with the values reported in [19].

A study of the dependence of the exponents δ_i on the notch angle ω_1 shows us more about the differences between particular bi-material classes. Let the angle $\omega_2 = -180°$ be fixed and the angle ω_1 changes in the interval $0 < \omega_1 < 180°$. The dependence of the exponents δ_i on the angle ω_1 for PZT-5H/BaTiO$_3$ bi-material is shown in Fig. 6.1(a). Similar behaviour can be obtained for all ε-class bi-materials. The eigenvalues δ_1 and δ_2 are real-valued almost in the whole interval $0 < \omega_1 < 180°$ except for the values $\omega_1 > 168°$, where they become complex conjugate. Note that the imaginary part of δ_2 is not plotted because it has the same values as $\Im\{\delta_1\}$ but with an opposite sign. The third eigenvalue δ_3 corresponds to the non-singular character of the stress and electric displacement field at the notch tip because $\delta_3 > 1$ up to $\omega_1 = 78°$ and it is always real. The real parts of complex conjugate eigenvalues δ_1 and δ_2 as well as the third eigenvalue δ_3 converge to the value 0.5 for $\omega_1 \to 180°$. It has to be pointed out that δ_3 is not equal to the real parts of neither δ_1 nor δ_2 for very closed notch configurations.

The same study was carried out for PZT-5H/PZT4 bi-material, one of representatives of the κ-class bi-materials. One can see in Fig. 6.1(b) the different dependency of the exponents δ_i on the ω_1 in contrast to the previous study. The third eigenvalue δ_3 provides the stress and electric displacement field at the notch tip, which is singular when $\delta_3 < 1$ for $\omega_1 > 75°$. Moreover, it is real-valued in the whole interval $0 < \omega_1 < 180°$. The exponents δ_1 and δ_2 are complex conjugate for $139° < \omega_1 < 166°$. For the interface crack as the limit case of the notch, the exponent δ_2 converges
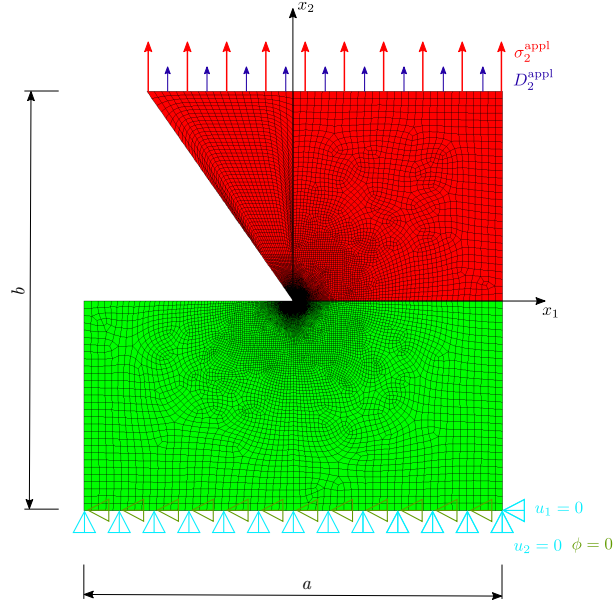
Fig. 6.2: Finite element mesh of the piezoelectric bi-material notch model with mechanical and electrical boundary conditions.

to 0.5, while the exponents δ_1 and δ_3 become symmetric with respect to the exponent δ_2. The same bi-material was investigated by Hirai et al. [6]. Unfortunately their results do not agree with our ones.

Comparing the graphs in Fig. 6.1 one can conclude that the bi-material classification introduced by Ou and Wu [19] for interface cracks cannot be applied to a bi-material notch with a geometry characterized by an arbitrary angle ω_1. Depending on the angle ω_1 both bi-materials PZT-5H/BaTiO$_3$ and PZT-5H/PZT-4 exhibit both the ε-class type and κ-class type behaviour. In the case of PZT-5H/PZT-4 bi-material there exists even a value range of ω_1 (139°, 166°) where simultaneously ε and κ differ from zero.

The knowledge of the character of the stress and electric displacement singularity represented by the exponents δ_i is necessary for the GSIFs evaluation discussed below. The FEM analysis is an important component of the procedure that allows one to get complete description of the singular stress and electric displacement field at the bi-material notch tip. The FEM results are obtained by using the codes of ANSYS and FEniCS. Both of them give the same results. The 8-node quadratic plane element `PLANE223` for coupled field analyses was used with the option of plane strain state (generalized plane strain and short circuit: $\varepsilon_3 = 0$ and $E_3 = 0$) in ANSYS. The notch geometry and boundary conditions are illustrated in Fig. 6.2.

At first, the path-independence of the Ψ-integral is tested. The values
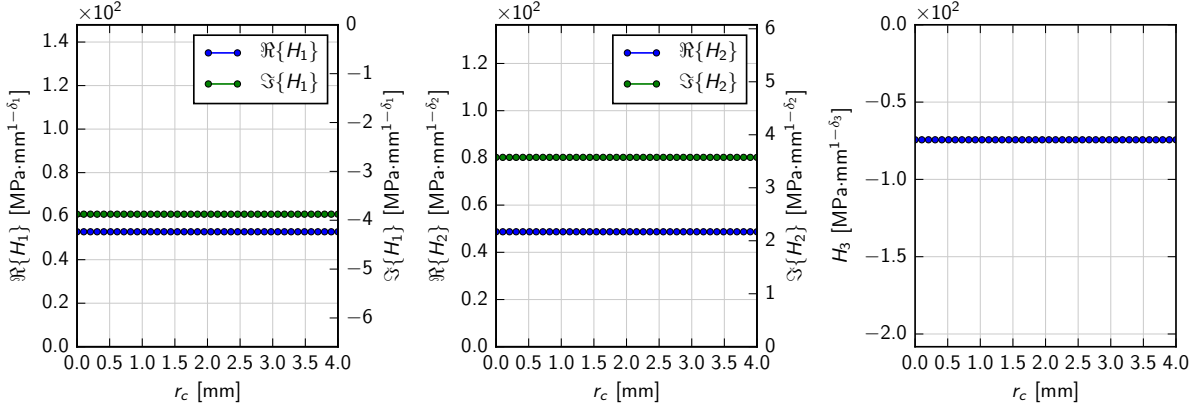
Fig. 6.3: Test of path-independence of the GSIFs on the integration contour radius enclosing the PZT-5H/BaTiO$_3$ piezoelectric interface crack with $\delta_1 = 0.5 + 0.01293i$, $\delta_2 = 0.5 - 0.01293i$, $\delta_3 = 0.5$.

of the GSIFs calculated via the Ψ-integrals (5.13) taken along circular contours with the radii $0.0005\,\text{mm} < r_c < 4\,\text{mm}$ are shown in Fig. 6.3. Hereinafter, the value $r_c = 2\,\text{mm}$ is chosen as the radius of the integration path of the Ψ-integrals in (5.13).

The asymptotic stresses and electric displacements can be written as

$$\begin{aligned}
\boldsymbol{\sigma}^1(r,\theta) &= - H_1 r^{\delta_1-1}\tilde{\boldsymbol{\lambda}}_{1,x_2}(\theta) - H_2 r^{\delta_2-1}\tilde{\boldsymbol{\lambda}}_{2,x_2}(\theta) - H_3 r^{\delta_3-1}\tilde{\boldsymbol{\lambda}}_{3,x_2}(\theta), \\
\boldsymbol{\sigma}^2(r,\theta) &= H_1 r^{\delta_1-1}\tilde{\boldsymbol{\lambda}}_{1,x_1}(\theta) + H_2 r^{\delta_2-1}\tilde{\boldsymbol{\lambda}}_{2,x_1}(\theta) + H_3 r^{\delta_3-1}\tilde{\boldsymbol{\lambda}}_{3,x_1}(\theta),
\end{aligned} \quad (6.3)$$

where

$$\boldsymbol{\sigma}^1 = \begin{Bmatrix} \sigma_{11} \\ \sigma_{12} \\ D_1 \end{Bmatrix}, \quad \boldsymbol{\sigma}^2 = \begin{Bmatrix} \sigma_{21} \\ \sigma_{22} \\ D_2 \end{Bmatrix}, \quad \tilde{\boldsymbol{\lambda}}_{,x_i}(x_1,x_2) = \frac{\mathrm{d}\tilde{\boldsymbol{\lambda}}(x_1,x_2)}{\mathrm{d}x_i}, \quad i = 1,2. \quad (6.4)$$

Let us consider poling directions $\alpha_1 = \alpha_2 = 90°$ and notch geometry $\omega_1 = 120°$ and $\omega_2 = -180°$. The asymptotic stresses, electric displacements, displacements and electric potentials calculated along the circular path with radius $r = 2\,\text{mm}$ encircling the notch tip in the bi-material PZT-5H/PZT-4 together with results obtained by FEM are shown in Fig. 6.4. The superscripts H_i, $i = 1,2,3$ of plotted quantities listed in the legend indicate particular asymptotic terms in Eqs. (3.5) and (6.3). The plots show a very good agreement of the asymptotic solution with the complete FEM solution obtained using a very fine mesh, which also demonstrates the accuracy of GSIFs calculations.

The stresses, electric displacements, displacements and electric potentials along the contour with the radius $r = 2\,\text{mm}$ encircling the interface crack tip in the bi-material PZT-5H/BaTiO$_3$ are shown in Fig. 6.5.
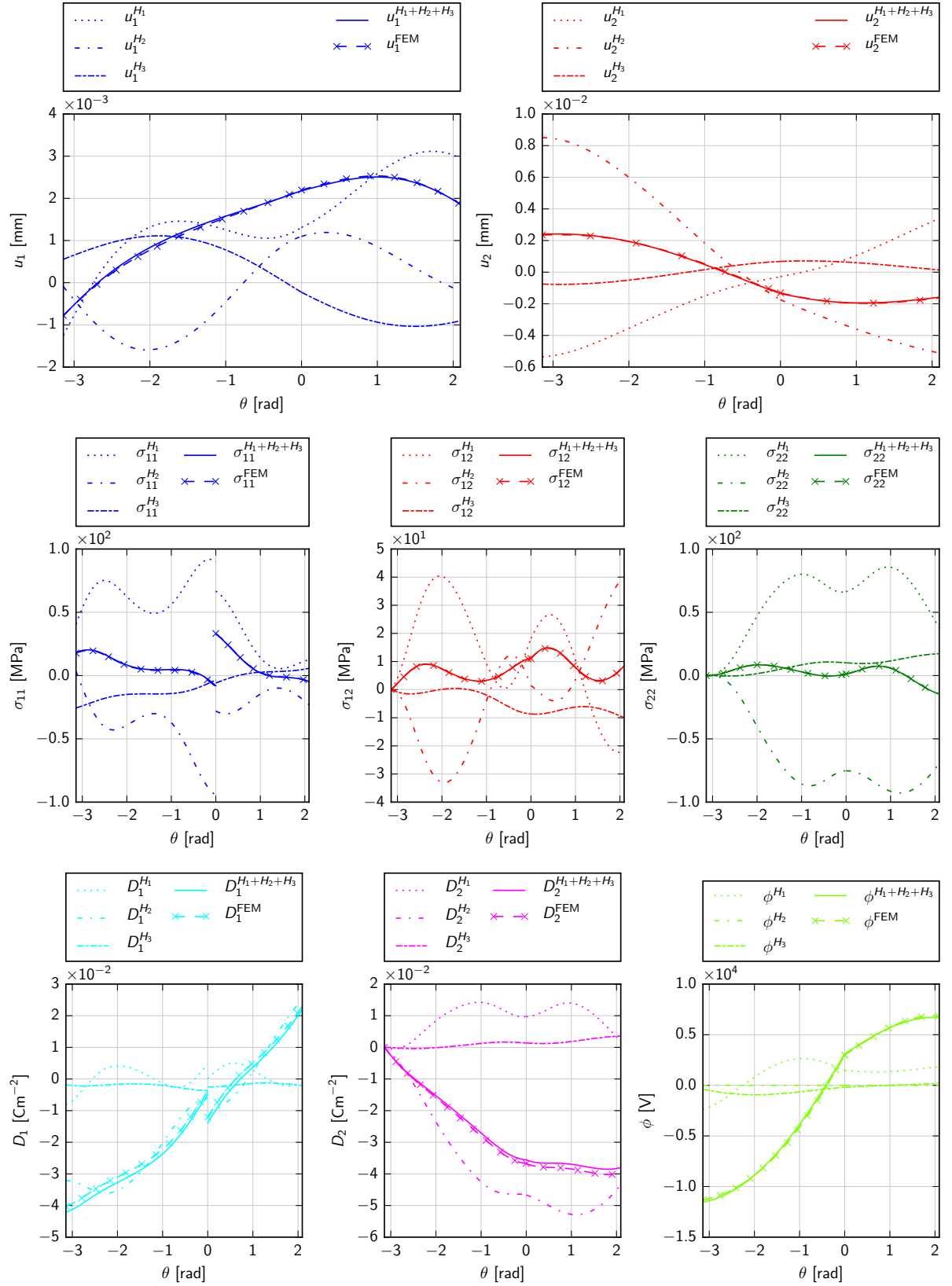
Fig. 6.4: The displacements, stress components, electric displacement components and electric potential of PZT-5H/PZT-4 bi-material notch on the circular path $r = 2\,\mathrm{mm}$, $\omega_1 = 120°$, $\omega_2 = -180°$, singularity exponents are $\delta_1 = 0.5154$, $\delta_2 = 0.5642$, $\delta_3 = 0.7299$.

23
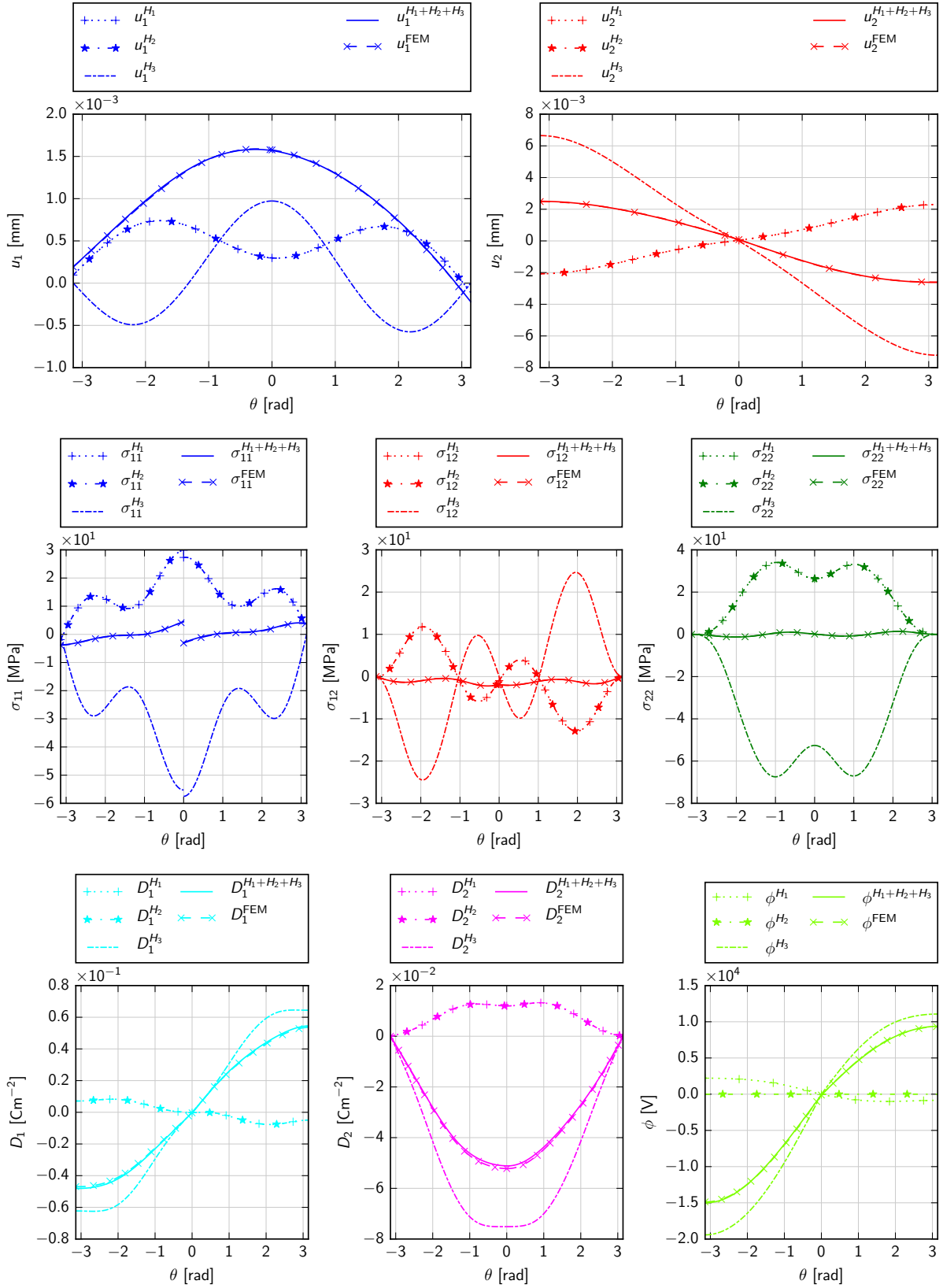
Fig. 6.5: The displacements, stress components, electric displacement components and electric potential of PZT-5H/BaTiO$_3$ bi-material notch on the circular path $r = 2\,\mathrm{mm}$, $\omega_1 = 180°$, $\omega_2 = -180°$, singularity exponents are $\delta_1 = 0.5 + 0.01293i$, $\delta_2 = 0.5 - 0.01293i$, $\delta_3 = 0.5$.

7 Conclusion

The determination of the singular stress behaviour is one of the necessary steps for life evaluation of constructions containing compound materials. The expanded Lekhnitskii-Eshelby-Stroh formalism for piezoelectric materials was applied to bi-material notches and interface crack problems. Although these two kinds of the stress concentrators are usually studied separately, especially in the case of the piezoelectric materials, the presented results showed that the used form of the expanded LES formalism captures acceptably both particular problems of the fracture mechanics. Additionally, the singularities of very closed bi-material notches, characterised by the complex valued exponents were part of the discussion. Also arbitrary poling orientation of the piezoelectric materials in the x_1x_2 plane was included into the considerations. The generalization of the so-called ε and κ classification of the piezoelectric bi-materials was suggested. It was ascertained that the exponents of the singularity of the stresses, mechanical and electric displacements and electric potential are independent of the parallel poling orientation of the bi-material. Although in the case of the interface crack the used exponent eigenvalue procedure is not able to distinguish between the real and complex exponent form as does the Hilbert problem formulation presented in Ou and Wu [19], it was shown that both methods give equivalent results. Finally, the Ψ-integral method was used to GSIF evaluation for various piezoelectric bi-material and notch configurations. After employing the improved numerical treatment of the ill-conditioned matrices in the piezoelectric constitutive law, the Ψ-integral path-independence was proved. The high accuracy of the GSIFs calculations was demonstrated by comparing the asymptotic solution with the complete FEM solution obtained using a very fine mesh. A future research will focus on proposal of fracture criteria based on extending the Finite Fracture Mechanics concept [35] to piezoelectric bi-material notches.

References

[1] HWU, Chyanbin. Some explicit expressions of extended Stroh formalism for two-dimensional piezoelectric anisotropic elasticity. *International Journal of Solids and Structures*. 2008, vol. 45, no. 16, pp. 4460–4473. ISSN 00207683.

[2] HWU, Chyanbin; IKEDA, T. Electromechanical fracture analysis for corners and cracks in piezoelectric materials. *International Journal of Solids and Structures*. 2008, vol. 45, no. 22-23, pp. 5744–5764. ISSN 00207683.

[3] HWU, Chyanbin; KUO, T.L. Interface corners in piezoelectric materials. *Acta Mechanica*. 2010, vol. 214, pp. 95–110.

[4] HWU, Chyanbin. *Anisotropic Elastic Plates*. 1st ed. New York: Springer US, 2010. ISBN 978-1-4419-5914-0.

[5] HWU, Chyanbin. A Unified Definition of Stress Intensity Factors for Cracks/Corners/Interface Cracks/Interface Corners in Anisotropic/Piezoelectric/Viscoelastic Materials. *Procedia Materials Science*. 2014, vol. 3, pp. 257–263. ISSN 22118128.

[6] HIRAI, H.; CHIBA, M.; ABE, M.; IKEDA, T.; MIYAZAKI, N. Stress intensity factor analysis of an interfacial corner between piezoelectric bimaterials using the H-integral method. *Engineering Fracture Mechanics*. 2012, vol. 82, pp. 60–72. ISBN 9780791844618. ISSN 00137944.

[7] ABE, M.; IKEDA, T.; KOGANEMARU, M.; MIYAZAKI, N. Stress intensity factor analysis of a three-dimensional interfacial corner between anisotropic piezoelectric multi-materials under several boundary conditions on the corner surfaces. *Engineering Fracture Mechanics*. 2017, vol. 171, pp. 1–21. ISSN 00137944.

[8] BELOKOPYTOVA, L.V.; FIL'SHTINSKII, L.A. Two-dimensional boundary value problem of electroelasticity for a piezoelectric medium with cuts. *J. Appl. Math. Mech.* 1979, vol. 43, pp. 147–153.

[9] SOSA, Horacio. Plane problems in piezoelectric media with defects. *Int. J. Solids Structures*. 1991, vol. 28, no. 4, pp. 491–505. ISBN 0020-7683. ISSN 02534827.

[10] CHEN, T. Further correspondences between plane piezoelectricity and generalized plane strain in elasticity. *Proceedings of the Royal Society A: Mathematical, Physical and Engineering Sciences*. 1998, vol. 454, no. 1971, pp. 873–884. ISSN 1364-5021.

[11] GAO, Cun-Fa; YU, Jian-Hang. Two-dimensional analysis of a semi-infinite crack in piezoelectric media. *Mechanics Research Communications*. 1998, vol. 25, no. 6, pp. 695–700. ISSN 0093-6413.

[12] XU, X.-L.; RAJAPAKSE, R.K.N.D. Analytical solution for an arbitrarily oriented void/crack and fracture of piezoceramics. *Acta Materialia.* 1999, vol. 47, no. 6, pp. 1735–1747. ISSN 13596454.

[13] HUANG, Zhenyu; KUANG, Zhen-Bang. Explicit expression of the A and B matrices for piezoelectric media. *Mechanics Research Communications.* 2000, vol. 27, no. 5, pp. 575–581. ISSN 0093-6413.

[14] XU, X.-L.; RAJAPAKSE, R.K.N.D. On singularities in composite piezoelectric wedges and junctions. *International Journal of Solids and Structures.* 2000, vol. 37, no. 23, pp. 3253–3275. ISSN 00207683.

[15] CHUE, Ching-Hwei; CHEN, Chung-De. Decoupled formulation of piezoelectric elasticity under generalized plane deformation and its application to wedge problems. *International Journal of Solids and Structures.* 2002, vol. 39, no. 12, pp. 3131–3158. ISSN 0020-7683.

[16] CHEN, Chung-De. On the singularities of the thermo-electro-elastic fields near the apex of a piezoelectric bonded wedge. *International Journal of Solids and Structures.* 2006, vol. 43, no. 5, pp. 957–981. ISSN 0020-7683.

[17] SUO, Zhigang. Singularities, interfaces and cracks in dissimilar anisotropic media. *Proceedings of the Royal Society A: Mathematical, Physical and Engineering Sciences.* 1990, pp. 331–358. ISSN 1364-5021.

[18] TIAN, Wen-Ye; CHEN, Yi-Heng. Interaction between an interface crack and subinterface microcracks in metal/piezoelectric bimaterials. *International Journal of Solids and Structures.* 2000, vol. 37, no. 52, pp. 7743–7757. ISSN 0020-7683.

[19] OU, Z.C.; WU, Xijia. On the crack-tip stress singularity of interfacial cracks in transversely isotropic piezoelectric bimaterials. *International Journal of Solids and Structures.* 2003, vol. 40, no. 26, pp. 7499–7511. ISSN 00207683.

[20] OU, Z.C.; CHEN, Y.H. Interface crack-tip generalized stress field and stress intensity factors in transversely isotropic piezoelectric bimaterials. *Mechanics Research Communications.* 2004, vol. 31, no. 4, pp. 421–428. ISSN 0093-6413.

[21] OU, Zhuo Cheng; CHEN, Yi Heng. Interface crack problem in elastic dielectric/piezoelectric bimaterials. *International Journal of Fracture.* 2004, vol. 130, no. 1, pp. 427–454. ISSN 03769429.

[22] SLÁDEK, J.; SLÁDEK, V.; WÜNSCHE, M.; ZHANG, Ch. Analysis of an interface crack between two dissimilar piezoelectric solids. *Engineering Fracture Mechanics.* 2012, vol. 89, pp. 114–127. ISSN 0013-7944.

[23] TING, T.C.T. *Anisotropic Elasticity : Theory and Applications.* New York: Oxford University Press, 1996. ISBN 1-280-52616-5.

[24] PROFANT, T.; KLUSÁK, J.; ŠEVEČEK, O.; HRSTKA, M.; KOTOUL, M. An energetic criterion for a micro-crack of finite length initiated in orthotropic bi-material notches. *Engineering Fracture Mechanics.* 2013, vol. 110, pp. 396–409. ISSN 00137944.

[25] BANKS-SILLS, Leslie; MOTOLA, Yael; SHEMESH, Lucy. The M-integral for calculating intensity factors of an impermeable crack in a piezoelectric material. *Engineering Fracture Mechanics.* 2008, vol. 75, no. 5, pp. 901–925. ISSN 00137944.

[26] QIN, Qing-Hua. *Advanced Mechanics of Piezoelectricity.* Beijing: Higher Education Press, 2013. ISBN 978-7-04-034497- 4.

[27] DESMORAT, R.; LECKIE, F.A. Singularities in bi-materials: parametric study of an isotropic/anisotropic joint. *European Journal of Mechanics - A/Solids.* 1998, vol. 17, no. 1, pp. 33–52. ISSN 09977538.

[28] ŠEVEČEK, Oldřich. *Solution of general stress concentrators in anisotropic media by combination of FEM and the complex potential theory.* 2009. Doctoral thesis. Brno University of Technology.

[29] PAPADAKIS, Panagiotis J.; BABUSKA, Ivo. A numerical procedure for the determination of certain quantities related to the stress intensity factors in two-dimensional elasticity. *Computer Methods in Applied Mechanics and Engineering.* 1995, vol. 122, no. 1-2, pp. 69–92. ISSN 0045-7825.

[30] SINCLAIR, G.B.; OKAJIMA, M.; GRIFFIN, J.H. Path independent integrals for computing stress intensity factors at sharp notches in elastic plates. *International Journal for Numerical Methods in Engineering.* 1984, vol. 20, no. 6, pp. 999–1008. ISSN 10970207.

[31] VU-QUOC, Loc; TRAN, Van Xuan. Singularity analysis and fracture energy-release rate for composites: Piecewise homogeneous-anisotropic materials. *Computer Methods in Applied Mechanics and Engineering.* 2006, vol. 195, no. 37-40, pp. 5162–5197. ISBN 0045-7825. ISSN 00457825.

[32] SOKOLNIKOFF, I.S. *Mathematical Theory of Elasticity.* New York: Tata McGraw-Hill, 1956.

[33] *ANSYS® Academic Research Mechanical, Release 18.1.*

[34] *FEniCS Project 2018.1.* Available also from: `https : / / feniscproject.org`.

[35] LEGUILLON, Dominique. Strength or toughness? A criterion for crack onset at a notch. *European Journal of Mechanics - A/Solids.* 2002, vol. 21, no. 1, pp. 61–72. ISSN 09977538.

Curriculum vitae

Personal details

Name	Ing. Miroslav Hrstka
Date of birth	24/02/1987
Address	Pod Kostelem 904, 696 04 Svatobořice-Mistřín
E-mail	Miroslav.Hrstka1@vutbr.cz

Education

09/2014 – 02/2015	Exchange Study, Erasmus+ (doctoral) *TU Darmstadt, Germany*
09/2012 – 06/2019	Applied Mechanics (doctoral) *Brno University of Technology* *Faculty of Mechanical Engineering* *Institute of Structural Mechanics*
09/2010 – 06/2012	Engineering Mechanics and Biomechanics (Ing.) *Brno University of Technology* *Faculty of Mechanical Engineering*
09/2007 – 06/2010	Fundamentals of Mechanical Engineering (Bc.) *Brno University of Technology* *Faculty of Mechanical Engineering*

Carrier overview

02/2017 – present	Numerical simulations engineer *Institute of Solid Mechanics, Mechatronics and Biomechanics, BUT*
01/2017 – 12/2018	Junior researcher *Central European Institute of Technology (CEITEC)*
03/2016 – 12/2018	Research student *Institute of Structural mechanics, Faculty of Civil Engineering BUT*
07/2012 – 09/2016	FEA Student engineer *Honeywell Technology Solutions, Brno*

Language skills

English (fluent) | German (fluent) | Czech (native)

Computer skills

Python, FORTRAN, LAPACK, ANSYS APDL, Linux, LaTeX, Autodesk, Inventor, Simulink

Abstract

The presented dissertation thesis deals with evaluation of the leading terms of the Williams asymptotic expansion describing an in-plane electro-elastic field at the tip of piezoelectric bi-material notches and interface cracks using the expanded Lekhnitskii-Eshelby-Stroh formalism in connection to the pure anisotropic elasticity. It is demonstrated that the expanded Lekhnitskii-Eshelby-Stroh formalism with modern Python programming concepts represents an effective theoretical as well as a practical tool for the fracture analysis of piezoelectric bi-materials. The governing equations focused on special types of monoclinic piezoelectric materials, which enable decoupling to the in-plane and anti-plane problem, are introduced via the complex potentials. In the practical part of the thesis, the eigenvalue problem of a bi-material notch is proposed in order to determine the singularity exponents as well as the generalized stress intensity factors by application of the two-state Ψ-integral. The accuracy of calculations of the generalised stress intensity factors is tested by comparing the asymptotic solutions with results obtained by the finite element method using a very fine mesh.

Abstrakt

Předkládaná dizertační práce se zabývá stanovením hlavních členů Williamsova asymptotického rozvoje popisujícího rovinné elektro-elastické pole v okolí piezoelektrických bi-materiálových vrubů a trhlin na rozhraní za použití rozšířeného Lechnického-Eshelbyho-Strohova formalismu v návaznosti na čistě anizotropní pružnost. Je ukázáno, že rozšířený Lechnického-Eshelbyho-Strohův formalismus představuje spolu s moderními programovacími koncepty v jazyku Python efektivní a také praktický nástroj pro lomovou analýzu piezoelektrických bi-materiálů. Základní rovnice zaměřené na speciální typy monoklinických materiálů, které umožňují oddělení rovinného a anti-rovinného problému, jsou vyjádřeny pomocí komplexních potenciálů. V praktické části práce je sestaven problém vlastního hodnot pro bi-materiálový vrub, na jehož základě jsou stanoveny exponenty singularity a pomocí dvoustavového Ψ-integrálu také zobecněné faktory intenzity napětí. Přesnost stanovení zobecněných faktorů intenzity napětí je testována srovnáním asymptotického řešení a řešení získaného pomocí metody konečných prvků s velmi jemnou sítí konečných prvků.